Hindawi
Journal of Nanomaterials
Volume 2021, Article ID 6628362, 12 pages
https://doi.org/10.1155/2021/6628362

Research Article

Antibacterial Filtration Using Polyethylene Terephthalate Filters Coated with Copper Nanoparticles

Vinh Tien Nguyen, Quang Hoang Anh Vu, Thi Ngoc Nhi Pham, and Khanh Son Trinh

Ho Chi Minh City University of Technology and Education, 01 Vo Van Ngan Street, Thu Duc District, Ho Chi Minh City, Vietnam

Correspondence should be addressed to Khanh Son Trinh; sontk@hcmute.edu.vn

Received 23 November 2020; Revised 7 January 2021; Accepted 16 January 2021; Published 27 January 2021

Academic Editor: Radu Claudiu Fierascu

The purpose of this study is to produce antibacterial filters based on a commercial polyethylene terephthalate (PET) filter with pores larger than bacterial cells. The antibacterial agent was copper nanoparticles (CuNP) which were synthesized and deposited on the PET filter by reducing copper(II) ions using sodium hypophosphite (NaH_2PO_2) as the reducing agent and polyvinylpyrrolidone (PVP) as the capping agent. Scanning electron microscopy coupled with energy-dispersive X-ray spectroscopy confirmed the presence of 150–300 nm CuNP on the surface of PET filters. We evaluated the amounts of deposited CuNP using a colorimetric method and the antibacterial-filtration capacity of CuNP/PET filters against *Escherichia coli* using the colony counting method. The reaction conditions were optimized successively using the one-factor-at-a-time approach for the concentration of copper precursor, the concentration of PVP, and the reaction time. The results showed that an initial 1 M $CuSO_4$, 0.8% *w*/*v* PVP, and 10-20 min of reaction resulted in a CuNP/PET filter with the highest antibacterial activity: 5.2 log cfu/mL reduction for *Escherichia coli* and 5.6 log cfu/mL reduction or *Staphylococcus aureus*. SEM images demonstrated the damages of the bacterial cells after passing through the CuNP/PET filter. ICP-MS analysis of the first liter of filtrate showed that the copper concentration of released copper was 0.6 ± 0.1 ppm, which is below the WHO standard for drinking water. Therefore, these CuNP/PET filters are promising for point-of-use disinfection of water, where clean potable water is not sufficient.

1. Introduction

The lack of safe drinking water is an increasing problem along with rapid population growth and industrialization in rural areas of developing countries [1]. Due to pollution and inappropriate and exploitation, the surface water and groundwater in these areas are usually contaminated with pathogens, which must be inactivated to provide safe potable water. To remove dissolved compounds and microorganisms, the common methods of water treatment are chemical precipitation followed by flocculation, sedimentation, or filtration. After removing the solids, chlorine is usually used to disinfect the water [2]. Due to toxicity and high reactivity, chlorine is not appropriate for household and point-of-use water purification systems at rural areas. Therefore, antibacterial filtration systems which can simultaneously remove solid particles and inactivate pathogens are desirable.

Nanomaterials are emerging as promising alternatives to traditional biocides due to their high effects and wide spectrum of inactivated bacteria. Silver is the most extensively studied nanomaterial for antimicrobial applications and were used in antibacterial filtration systems ([3]; Theresa A Dankovich, Levine, Potgieter, Dillingham, & Smith, 2016). However, the high cost of silver is its main disadvantage. Copper and copper oxide nanoparticles have lower production cost and relatively high antimicrobial effects on a wide range of microorganisms and thus can be used to replace silver nanoparticles in antimicrobial applications [4–6]. The antimicrobial effects of metal and metal nanoparticles generally are attributed to their small sizes, high surface-to-volume ratios, and the ability to release metal ions into solution. All these factors allow nanoparticles to interact, directly and indirectly, with microbial cells. It should be noted that the main drawback of copper nanoparticles (CuNP) that hinders its

practical applications until now is its high tendency to be oxidized to copper oxides when exposed to air due to their high surface activity.

There have been many studies on the synthesis of copper nanoparticles using various reducing agents such as hydrazine, ascorbic acid, and sodium borohydride. However, the downsides of sodium borohydride and hydrazine are their instability and toxicity. Ascorbic acid, also known as vitamin C, is a green, safe, and mild reducing agent that can reduce copper ions to metallic copper and stabilize the formed CuNP (Theresa A. Dankovich & Smith, 2014; [7]). The main disadvantage of ascorbic acid is its high cost. Sodium hypophosphite NaH_2PO_2 is also a safe and mild reducing agent, but much cheaper compared to ascorbic acid [8]. Therefore, in this study, we used NaH_2PO_2 to reduce copper ions to CuNPs. In addition, polyvinylpyrrolidone (PVP) was also used to prevent aggregation of the formed CuNPs [5].

For practical antibacterial applications, nanomaterials are usually deposited on solid surfaces such as glass, ceramics, or polymers [9]. Polyethylene terephthalate (PET) is polyester with high tensile strength, wash and wear stability, and resistance to many chemicals. To widen the applications of PET materials, the wetting properties of its surface can be altered by attaching conductive materials [10], coating with hydrophilic polymers [11], or alkaline etching (Hsieh, Miller, & Thompson, 1996). The latter approach is preferable due to its simplicity and ease of upscaling.

In this study, we pretreated PET filters with concentrated KOH before synthesizing and depositing CuNP onto their surfaces by reducing $CuSO_4$ with ascorbic acid in the presence of PVP as the capping agent. Triethanolamine (TEA) was also employed to improve the surface activity of PET fibers due to the aminolysis of the polyester [12]. The reaction conditions, including concentrations of $CuSO_4$ and PVP, as well as the reation time, were initially optimized using the antibacterial filtration capacity of the CuNP/PET filters against *Escherichia coli* as the optimizing criterion. Other aspects of the CuNP/PET filters, including the size distribution of the deposited CuNP, the mechanism of antibacterial filtration, and concentration of copper released in the filtrate, were evaluated.

2. Materials and Method

2.1. Materials. PET filters were purchased at Dong Chau Environmental Construction Co., Ltd. (Vietnam) with the following specifications: 25 μm average pore size, 3.6 g/cm^2 grammage, 2.2 mm thickness, 65-85 m^3/m^2/min air permeability, working pH 4-12, and working temperature < 130°C.

Escherichia coli and *Staphylococcus aureus* were purchased at the Library of Microbiological Genes under the Institute of Microbiology and Biotechnology–Hanoi National University.

All chemicals were purchased from Xilong Scientific Ltd. (China) with analytical grades and used as received.

2.2. Experimental Design. CuNPs were chemically prepared and deposited on PET filters, which were then evaluated based on the amount of deposited CuNP and their antibacterial ability against the Gram-negative *E. coli*. To optimize the antibacterial-filtration capacity of CuNP/PET filters for a reasonable cost, the one-factor-at-a-time experimental design was used for initial $CuSO_4$ concentration, PVP concentration, and reaction time. The optimal CuNP/PET filter was then analyzed using a scanning electron microscope coupled with energy-dispersive X-ray spectroscopy (SEM-EDX) for characterization and inductively coupled plasma mass spectrometry (ICP–MS) for copper release evaluation. Moreover, the bacterial cells were observed using SEM to evaluate their morphological changes after being passed through the optimal CuNP/PET filter.

2.3. Preparation of CuNP/PET Filters. CuNP were synthesized according to a published method with some modifications [5]. PET filters were pretreated by immersing in a 10 M KOH solution for 60 min. The filters were then thoroughly washed with distilled water until neutral. After being dried at room temperature, each alkaline-treated PET filter was immersed in a mixture of 48 mL of 0.68% w/v NaH_2PO_2 and 0.42–1.4% w/v PVP solution and 1 mL of 0.4–1.0 M $CuSO_4$ solution. The reaction mixture was heated in a boiling water bath for 15 min. One milliliter of TEA was then added to the mixture. The mixture was then heated again in the boiling water bath for 45 min. The filters were then washed several times with distilled water for complete removal of solutes and unbound CuNP. The filters were then dried at 40–50°C for 8 h and stored in a plastic bag.

2.4. Relative Mass Loss of KOH-Treated PET Filters. Relative mass loss of PET filter was evaluated by weighing the PET filter before and after immersed in the 10 M KOH solution for 30, 60, 90, or 135 min. All PET samples after alkaline treatment were rinsed with distilled water to eliminate KOH and dried at 60°C for 3 h before being weighted. The relative mass loss of PET filter was calculated as follows:

$$\mathrm{RM} = \frac{m_i}{m_a} \times 100, \tag{1}$$

where RM is the relative mass loss (%), m_i is the initial weight of PET filter (g), and m_a is the weight of PET filter after treated with 10 M KOH.

2.5. Quantitative Analysis of Deposited Copper on CuNP/PET Filters. The amount of copper deposited on each PET filter was quantified using a colorimetric method (Yoe & Barton, 1940). Each CuNP/PET filter was immersed in a solution containing 6 mL of 2 M HNO_3 at 70°C for 10 min to convert all CuNPs and copper oxides into Cu^{2+} ions:

$$\begin{aligned} 3\,\mathrm{Cu} + 8\,\mathrm{HNO_3} &\longrightarrow 3\,\mathrm{Cu(NO_3)_2} + 2\,\mathrm{NO} + 4\,\mathrm{H_2O} \\ \mathrm{CuO} + 2\,\mathrm{HNO_3} &\longrightarrow \mathrm{Cu(NO_3)_2} + \mathrm{H_2O} \\ 3\,\mathrm{Cu_2O} + 14\,\mathrm{HNO_3} &\longrightarrow 6\,\mathrm{Cu(NO_3)_2} + 7\,\mathrm{H_2O} + 2\,\mathrm{NO} \end{aligned} \tag{2}$$

The PET filter was then rinsed with small portions of distilled water to remove remaining solutes. The solution after boiling and the portions of rinsing water were combined,

neutralized with 3.5 mL of 3 M KOH, and complexed with 3 mL of 0.5 M TEA to form a dark blue complex solution. The copper concentration in the solution was determined by measuring its absorbance at 650 nm and referring to a standard curve (Figure 1) built from $Cu(NO_3)_2$ and TEA.

2.6. Antibacterial Effects of CuNP/PET Filters. *E. coli* and *S. aureus* previously stored at 4°C were incubated on nutrient broth (NB) medium for 24 h at 37°C. After that, the bacterial suspension was successively diluted 10-fold with a 0.9% (*w*/*v*) NaCl solution to a series of suspensions with 10-, 10^2-, 10^3-, 10^4-, and 10^5-fold dilution. Each suspension (100 μL) was spread on NB agar on Petri dishes and incubated for 24 h at 37°C. The diluted suspension with an optimal number of colonies (between 25 and 250 [13]) was chosen as the origin to calculate bacterial densities (in cfu/mL) in the other suspensions by multiplying with 10 (to convert from 100 μL to 1 mL) and then with the dilution factor.

A bacterial suspension (10^3-10^5 cfu/mL, approximately 8 mL) was passed through each filter at 0.53 mL/min for 15 min. The bacterial densities in the suspension before and after passing through the filter were determined by the diluting, spreading, incubating, and colony counting techniques mentioned above. The antibacterial test was triplicated for each CuNP/PET filter and the control PET filter.

Antimicrobial-filtration capacities of CuNP/PET filters are expressed as the reduction in log cfu/mL of bacterial cell density or percent of inactivation as follows:

$$\log \text{reduction} = \log A_1 - \log A_2, \quad (3)$$

where log reduction is the reduction in logarithm of bacterial density (log cfu/mL), A_1 is the bacterial density before filtration (cfu/mL), and A_2 is the bacterial density in the filtrate (cfu/mL).

2.7. Morphology and Size Distribution of CuNP. SEM-EDX (S–4800 model, Hitachi, Japan) was used to confirm the presence of copper and to evaluate the morphology and size distribution of CuNP deposited on PET filters. To build the size distribution of CuNP, the sizes of 150 particles from the SEM images were measured using ImageJ software (version 1.49u).

2.8. Morphology of E. coli after Passing through CuNP/PET Filters. The morphology and damages of bacteria cells before and after filtering through the optimal CuNP/PET were evaluated using SEM after a series of bacterial cell treatments [14, 15]. Each bacterial suspension was transferred onto a square glass slide (1 cm^2) by a sterile inoculation loop and one drop of 2.5% glutaraldehyde solution was added. The glass slide was then put inside a closed sterile Petri dish and left for 24 h at 37°C to fix the bacterial cells. The cells were then gradually dehydrated by successive immersion for 10 min in each ethanol solution with increasing concentrations (30, 50, 70, 90, and 100% *v*/*v*). After air drying, the glass slide was coated with platinum for SEM recording.

2.9. Evaluation of Copper Release from CuNP/PET Filters. Deionized water (1 L) passed through the CuNP/PET filter at a speed of 0.53 mL/min. The water samples before and after filtration were acidified with HNO_3 and analyzed using ICP–MS to evaluate the amount of copper released from the filter.

2.10. Statistical Analysis. The significant difference between experimental data was analyzed with ANOVA using SPSS software (version 20.0, USA).

3. Results and Discussion

3.1. Relative Mass Loss of PET Filters during KOH Treatment. We found that the original PET filters could not hold the formed CuNP, while a KOH treatment of the filters significantly enhances their surface attachment toward CuNP. The mechanism behind this phenomenon is the hydrolysis of PET fiber surface in the alkaline solution, resulting in the formation of carboxylate groups, which can bind copper ions and hold CuNP.

To find an appropriate time of KOH treatment, we measured the relative mass loss of PET filters over treatment time (Figure 2). The relative mass loss increased almost linearly with treatment time from 30 to 120 min.

The original PET fiber surface was smooth (Figure 3(a)), while there were many holes with diameters of 0.5–2.0 μm on the fiber after 60 min of KOH treatment (arrows on Figure 3(b)).

In KOH solutions, PET is partially hydrolyzed into soluble ethylene glycol, potassium terephthalate, and short-chain fragments, hence reducing the weight of the filter and forming the holes on the PET fiber surface (Figure 4). These holes, where the polymer was hydrolytically cleaved, contain carboxylate and hydroxyl groups which may interact and bind copper ions more effectively than the untreated fiber surface [16].

We found that a treatment time longer than 120 min severely deteriorated the filter, making it mechanically very weak. Therefore, 60 min was chosen as the appropriate time of KOH treatment before CuNP deposition.

3.2. CuNP/PET Filter Preparation: Influence of Copper Precursor Concentration. We first optimized the concentration of $CuSO_4$ based on the amount of copper deposited on PET filters (Figure 5). The grey and black colors of these filters were due to the quick oxidation of CuNP to a surface CuO layer upon contact with the air [17]. When the $CuSO_4$ concentration increased from 0.4 to 1.4 M, the CuNP/PET filters turned from grey to black (Figure 5(a)), corresponding to an increase in the density of CuNP deposited on the filters (Figure 5(b)).

The amount of deposited CuNP reached a maximum of approximately 2.1 mg/cm^2 with the initial 1.0 M $CuSO_4$ solution. This value was 10000 times higher than the maximum copper density in a similar study (2.04×10^{-4} mg/cm^2), possibly due to the alkaline pretreatment in our study [18]. No statistical difference was found between CuNP/PET filters obtained with $CuSO_4$ concentrations from 1.0 to 1.4 M. Therefore, for economical reason, we chose 1.0 M as the optimum $CuSO_4$ concentration to prepare CuNP/PET filters.

The antimicrobial ability against *E. coli* was investigated on the CuNP/PET filters above, which contained different

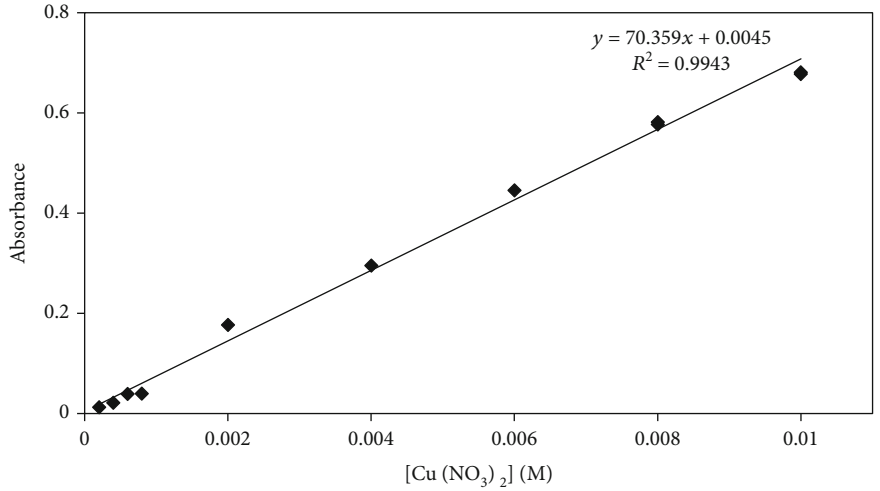

Figure 1: Standard curve of $Cu(NO_3)_2$–TEA complex at measured at 650 nm.

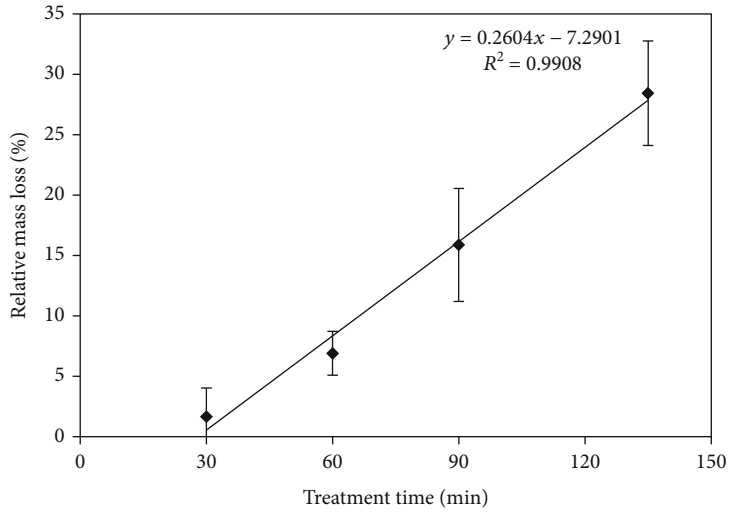

Figure 2: Relative mass loss of PET filter treated with 10 M KOH.

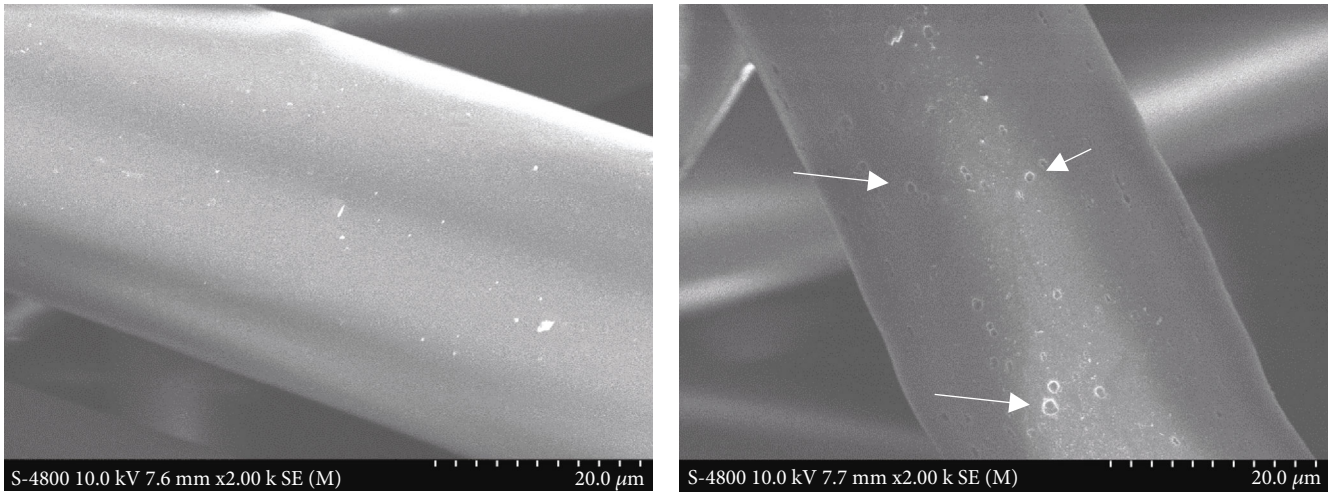

(a) (b)

Figure 3: SEM image of PET fibers before (a) and after immersion in alkaline solution for 60 min (b).

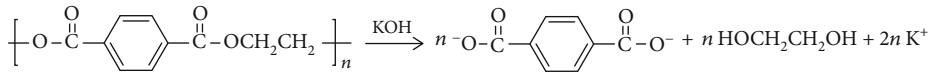

Figure 4: Hydrolysis of PET by KOH solution.

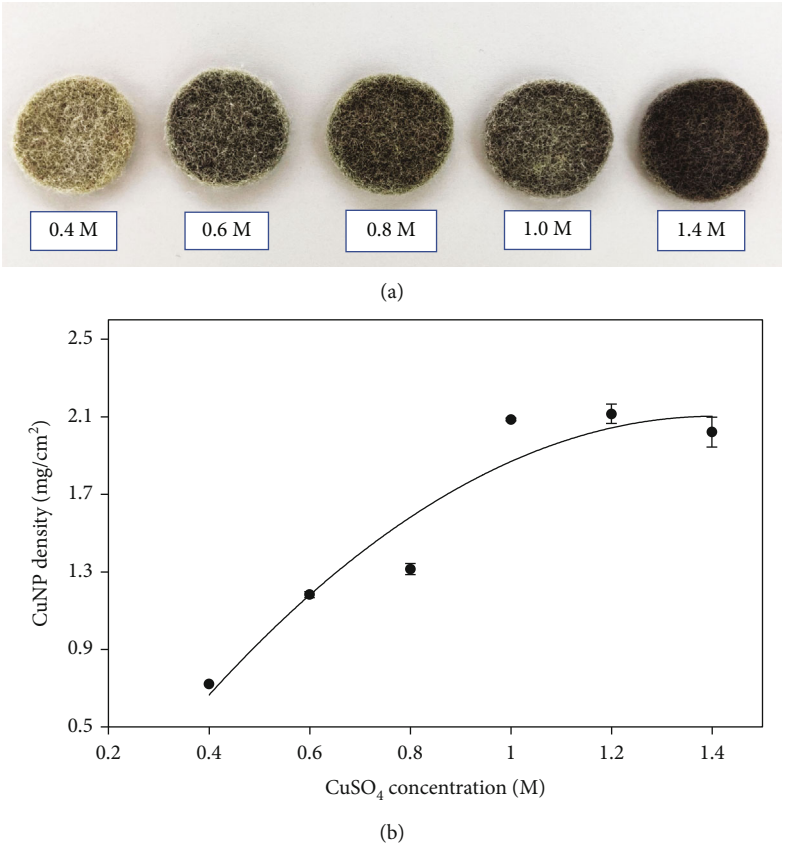

Figure 5: Appearance (a) and copper density (b) of CuNP/PET filters prepared with different concentrations of $CuSO_4$; 0.42% *w*/*v* PVP, 45 min of reaction.

amounts of CuNPs. Suspensions of *E. coli* with cell densities from 3.5 to 5.0 log cfu/mL were passed through the filters. The control PET filter did not exhibit any significant inhibition because its pore size (25 μm) is much higher than the size of *E. coli* (1.0-2.0 μm) (Council, 1999). Figure 6 shows that higher amounts of CuNP deposited on PET filters resulted in higher bacterial inhibition. This relationship can be explained by the greater amount of Cu^{2+} ion released into the suspension and higher direct contacts between bacterial cells and CuNP during filtration when more CuNPs are present on the filter.

For the sake of comparison, we converted the copper content of 2.1 mg/cm^2 to 0.58 mg/g using the 3.6 g/cm^2 grammage of the filter. This copper content resulted in a 3.5 log reduction in *E. coli* density, which was comparable with that in a previous study (Theresa A. Dankovich & Smith, 2014). In the study, CuNP deposited on blotting paper with a density of 10 mg/g, which is approximately 17 times higher than ours, exhibited a 4.6 log reduction, which is approximately 13 times higher than ours.

The antibacterial effect of copper ions is the result of a series of their actions: binding and changing the permeability of the cell membrane, penetrating through channels, altering DNA structure of bacteria, interfering with mitosis, and ultimately inactivating and destroying bacteria [19]. Another possible explanation is when the bacteria suspension passed through the CuNP/PET fibers with a high density of surface CuNP, the bacterial cells can collide with the CuNP, leading to cell membrane damages and the formation of reactive complexes between CuNP and biological components in the cell [18].

3.3. CuNP/PET Filter Preparation: Influence of Capping Agent Concentration. It is well known that capping agents play a vital role in the synthesis of nanomaterials by controlling sizes of the formed particles. Moreover, we found that the concentration of the capping agent (PVP) influences the amount of CuNP deposited on PET filters (Figure 7).

The CuNP density on PET filters increases with PVP concentration in the 0.4–1.0% *w*/*v* range and reaches a

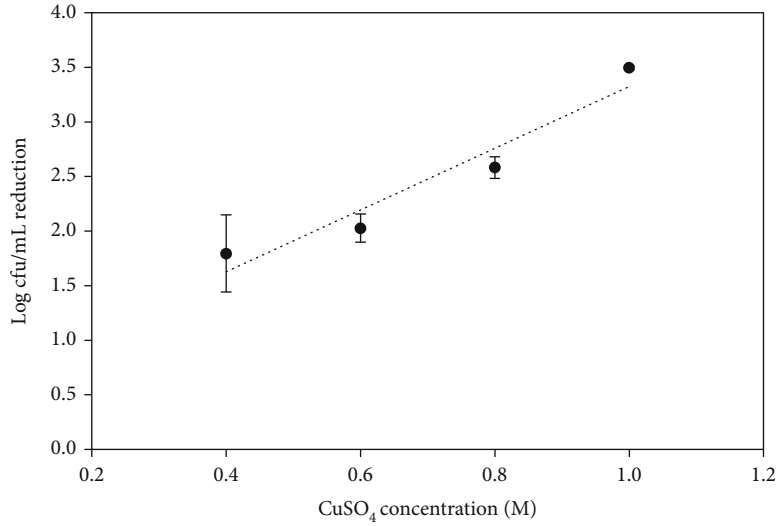

Figure 6: Log reduction of E. coli in suspensions after passing through CuNP/PET filters at different initial concentrations of $CuSO_4$.

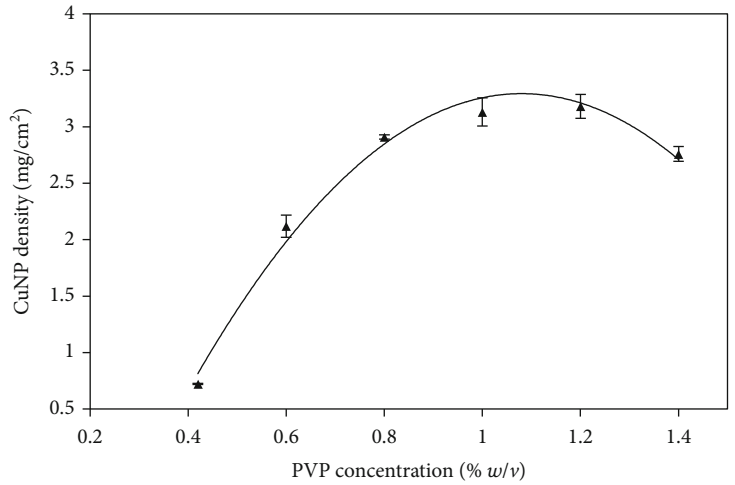

Figure 7: Influence of PVP concentration on the density of CuNP deposited on PET filters; 1 M $CuSO_4$, 45 min of reaction.

maximum at 1.0–1.2%. A possible explanation for this result is that PVP molecules cap the formed CuNP, hence preventing their agglomeration and keeping their sizes small. The small sizes of CuNP result in their high surface energy and a tendency to be adsorbed on the PET fibers. However, when the capping agent concentration is too high, the PVP capping layer on the CuNP becomes too thick and prevents the nanoparticles to deposit on the PET filter.

In our study, the highest antimicrobial ability (3.0 log reduction) of CuNP/PET filters was reached for the 0.8% PVP filter (Figure 8), while the 1.0% PVP filter with a higher CuNP density showed a lower bacteria inactivation (2.80 log reduction). This unexpected reverse correlation between CuNP density and antibacterial effect can be explained by the presence of the thick capping layer on the CuNP surface at 1.0% PVP, which hindered the release of copper ions and thereby reduced their antimicrobial ability. This hypothesis is supported by the result in another research, in which PVP at a high concentration interfered with silver release from silver nanoparticles and decreased their antibacterial capacity [20]. Therefore, we chose 0.8% *w*/*v* as the optimal PVP concentration to prepare antibacterial CuNP/PET filters.

3.4. CuNP/PET Filter Preparation: Influence of Reaction Time. The process of reducing Cu^{2+} ion to CuNP starts from the reaction of NaH_2PO_2 with water molecules at approximately 100°C to create hydrogen atoms [21]:

$$H_2PO_2^- + H_2O \longrightarrow H_2PO_3^- + 2H \quad (4)$$

These hydrogen atoms then transfer electrons to Cu^{2+} ions to produce Cu in two stages: from Cu^{2+} to Cu^+ and then from Cu^+ to Cu^o [22]. The color of CuNP/PET filters changed with reaction time. In the first stage (10 min from the moment of TEA addition), the solution changes from blue to dark yellow, indicating the formation of Cu_2O nanoparticles. In the second stage (within 35 min after the first stage),

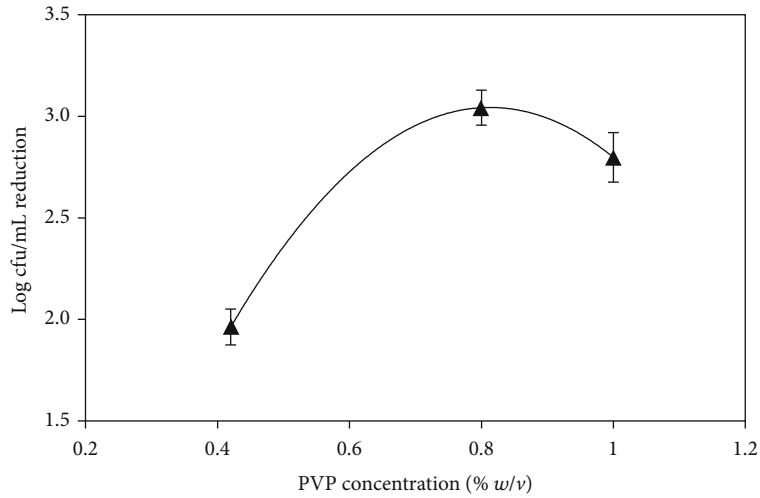

Figure 8: Reduction of E. coli density in suspensions after passing through CuNP/PET filters prepared with different PVP contents.

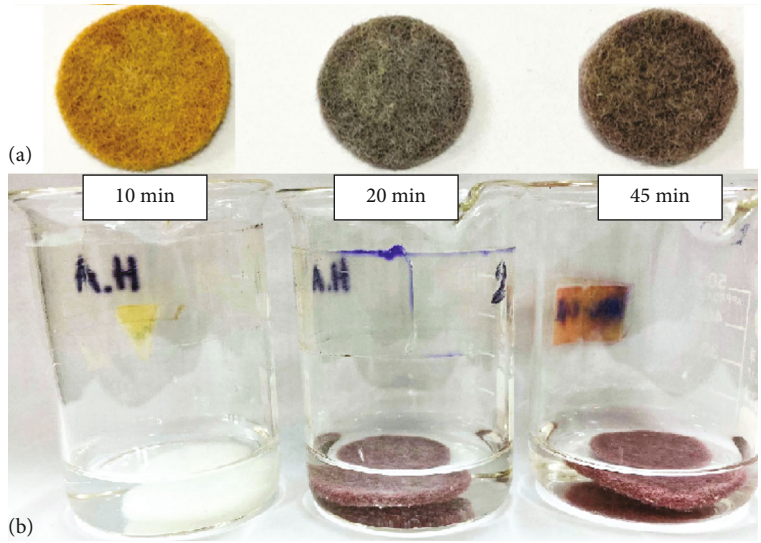

Figure 9: Color of PET filters when (a) exposed to air after different reduction time and (b) subsequently immersed in 0.1 M HCl.

the solution changes from dark yellow to brick red, indicating the formation of CuNP.

In the first stage, the newly formed Cu_2O nanoparticles attached to the holes on the PET surface and served as nuclei. In the second stage, Cu_2O were reduced to Cu and more Cu_2O nanoparticles are formed and cling to existing nuclei, leading to an increase in particle size. In this process, the polymeric capping agent (PVP) prevents the aggregation of the nanoparticles and keeps them in the nanoscale sizes [5].

Figure 9(a) shows that the 10 min filter turns from white to yellow, indicating the dominant presence of Cu_2O on its surface. After 20 min and longer time, the yellow color turned mainly black due to the reduction of Cu_2O to Cu and the quick subsequent oxidation of the CuNP to CuO when exposed to air. To verify this hypothesis, the filters in Figure 9(a) were immersed in 10 mL of 0.1 M HCl solution, which resulted in immediate color changes (Figure 9(b)). The yellow 10 min filter turned white due to the disproportionation and dissolution of Cu_2O in the acidic solution. The black 20 min and 45 min filters turned brick-red, indicating the presence of metallic copper under the CuO layer.

Interestingly, the PET filters after 10 min of reducing copper ions demonstrated antibacterial activity stronger than those obtained after 20 and 45 min of reduction (Figure 10(a)).

The highest antibacterial effect of the 10 min filter was due to the nature of nanoparticles on the filter surface: Cu_2O possesses higher antibacterial potency than CuO nanoparticles [4, 23–25]. When the time of Cu^{2+} reduction increased to 20 and 45 min, the antibacterial effect of the filter decreased (Figure 10(a)) because Cu_2O was gradually converted to Cu, which was then quickly oxidized in the air to CuO with lower antibacterial potency. This result is interesting because it suggests that coating PET filters with solely Cu_2O may result in even higher antibacterial effects. It should be noted that Cu_2O nanoparticles are more stable than CuNP

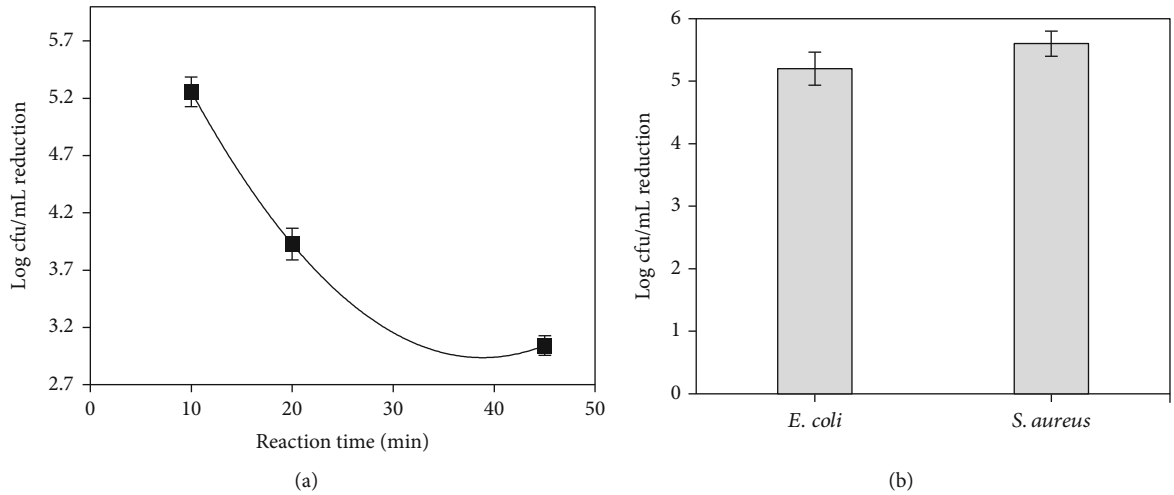

Figure 10: (a) Log reduction of E. coli suspensions after passing through CuNP/PET filters prepared with different reaction times. (b) Antibacterial effects of the 10 min filter on E. coli and S. aureus.

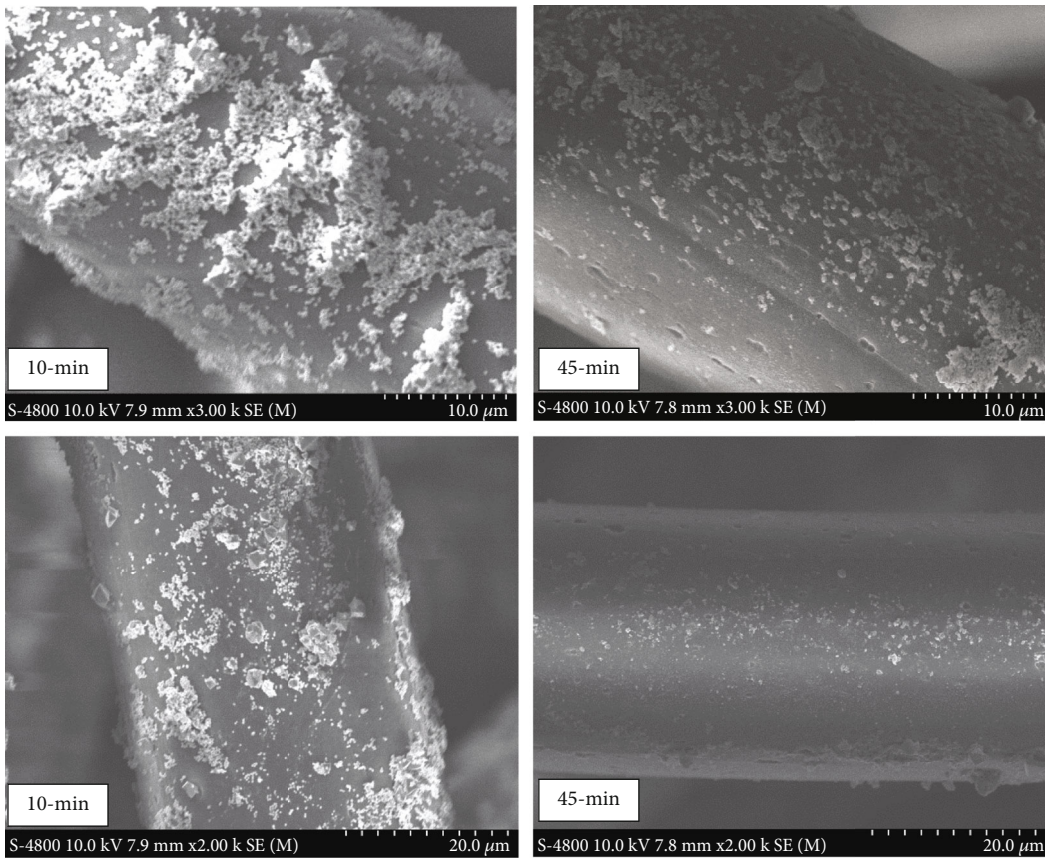

Figure 11: SEM micrograph of the 10 min and 45 min filters at different magnifications.

and can be synthesized easily using inexpensive and nontoxic agents, such as reducing sugars and plant extracts [26, 27].

There are several possible antibacterial mechanisms of nanoparticles of copper oxides. The first mechanism is related to the copper ions released from the surface of the oxide nanoparticles. Compared to CuO, Cu_2O has higher solubility and release rate of copper ions, and thus higher antibacterial effect [23]. The second possible mechanism is contact killing, where bacterial cells collide with the copper oxide nanoparticles. After getting contact with the bacterial cell wall, the nanoparticles can alter the permeability of the cell membrane, interact with proteins and DNA, and inactivate enzymes, and the final result is the cell destruction [24].

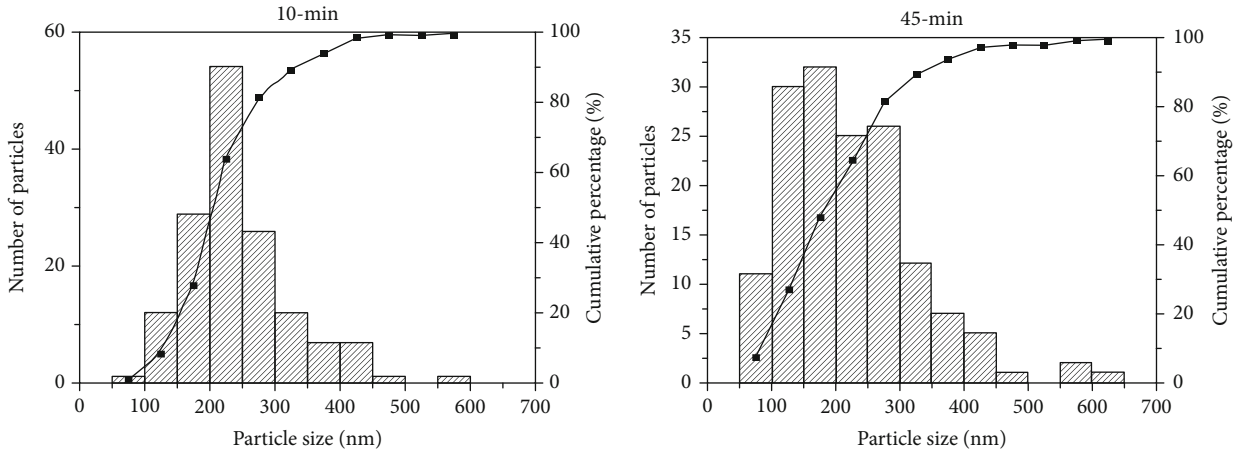

Figure 12: Size distribution of CuNP deposited on the 10 min and 45 min filters.

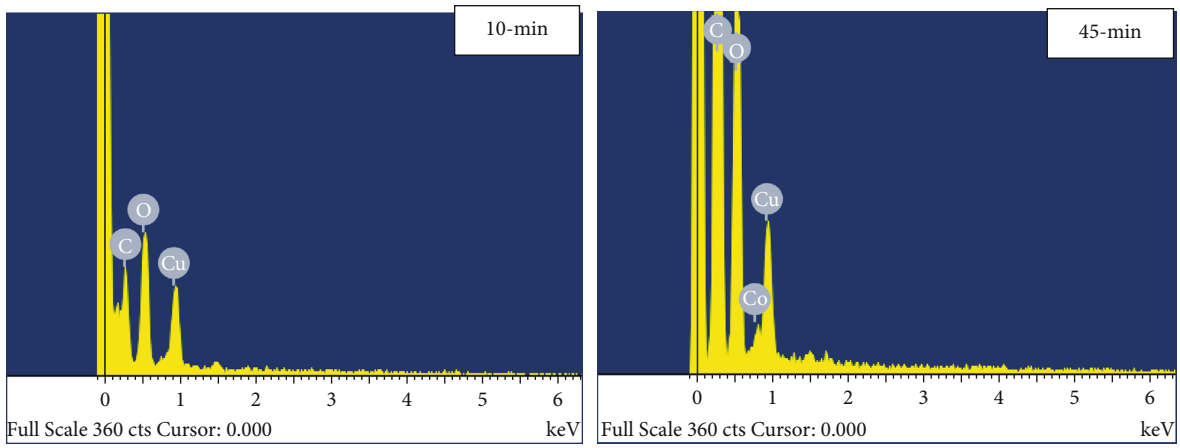

Figure 13: EDX spectra of an area on the surface of the 10 min and 45 min filters.

In addition to the Gram-negative *E. coli*, the antibacterial effect of the 10 min filter was also tested on the Gram-positive *S. aureus*. Figure 10(b) showed a 5.6 log reduction for *S. aureus* in comparison with the 5.2 log reduction for *E. coli*. This result agrees with previous works confirming that the antibacterial abilities of metal nanoparticles on Gram-positive bacteria are stronger than on Gram-negative bacteria [28, 29]. This can be explained based on the difference in the cell membrane compositions of these bacteria [30]. According to these authors, the cell wall of *S. aureus* has no outer membrane and has a thick (20–80 nm) peptidoglycan membrane containing negatively charged moieties of teichoic acid, giving *S. aureus* a higher affinity for positively charged metal ions than *E. coli*.

All the above results showed that a 10 min filter (mainly composed of Cu_2O nanoparticles) has a higher antimicrobial ability against *S. aureus* than *E. coli*. Therefore, we chose the 10 min and the 45 min filters to evaluate the size, distribution, and morphology of CuNP.

3.5. Morphology, Size, and Distribution of CuNP. SEM micrographs of the 10 min and 45 min filters (Figure 11) show that the CuNP on the filter surface form clusters. The clusters on the 10 min filter were more porous, while the clusters on the 45 min filter were more compact. We suggest that the high porosity of CuNP clusters on the 10 min filter may play a role in its stronger release of copper ions and higher antibacterial activity.

Table 1: Surface elemental composition of the 10 min and 45 min filters.

	Atomic composition (%)	
	10 min filter	45 min filter
C	45.17	56.15
O	46.58	35.35
Cu	8.25	8.50

Figure 12 shows the size distribution of CuNP on the 10 min and 45 min filters. There was no significant difference between their ranges of particle sizes, which were from 50 to 600 nm. The peak in the size distribution for the 10 min filter was sharper, indicating a monodispersity higher than that of the 45 min filter. The higher polydispersity for the 45 min filter can be explained by the longer reaction time results in Ostwald ripening of CuNP, in which smaller particles dissolve and redeposit on larger particles.

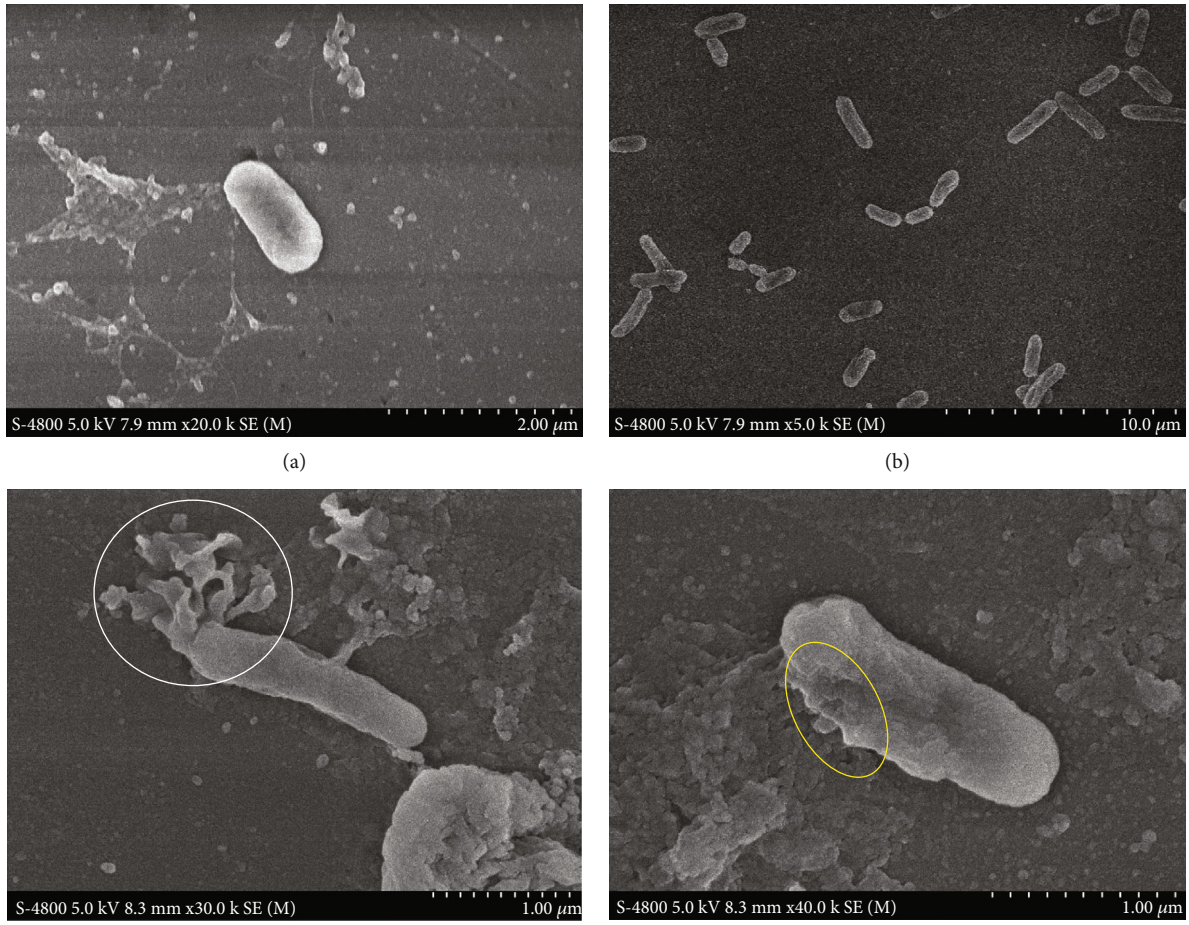

Figure 14: E. coli cells before (a, b) and after (c, d) passing through the 10 min filter.

For both filters, approximately 75% of CuNPs were between 100 and 300 nm, which is larger than the average size in other studies [5, 21]. Although large sizes associate with a slower release of copper ions and lower antibacterial effects, the high density of CuNP on the filters can compensate for this disadvantage. From a practical point of view, larger CuNP size and slower ion release make the filter serviceable for a longer time.

The presence of copper on filters was confirmed by its characteristic peak in the EDX spectra (Figure 13). The atomic% of oxygen on the 45 min filter was lower than that on the 10 min filter (Table 1), indicating the conversion of Cu_2O to Cu during the reaction.

Because each $C_{10}H_8O_4$ monomeric unit of PET contains 14 atoms of carbon and oxygen, the 8% of atomic copper content means an average $Cu/C_{10}H_8O_4$ ratio of 1.2 : 1 or each PET monomeric unit attach 1.2 copper atom. This high average density of copper explains the high antibacterial activity of the CuNP/PET filters.

3.6. Morphology of E. coli after Passing through the Optimal 10 min CuNP/PET Filter. To evaluate the morphological changes of the *E. coli* cells after being filtered through the optimal 10 min filter, the cells were observed using SEM after a series of sample treatment described in the experimental section (Figure 14).

After being filtered through the 10 min filter, the *E. coli* cells were shrunk (yellow circle in Figure 14(d)) and completely ruptured (white circle in Figure 14(c)) as compared to the smooth surface of the untreated *E. coli* cells (Figures 14(a) and 14(b)). The rupture of *E. coli* cells was mainly caused by the influence of CuNP. Similar morphological changes in bacterial cells were observed in many research on antibacterial effects of nanomaterials [31–33]. These results indicate that CuNP on PET filters were responsible for bacterial cell death by deforming and breaking the cell wall.

The shrinkage of *E. coli* cells can be explained based on the ability of CuNP to change the permeability of bacterial cell walls. Specifically, when *E. coli* cells mechanically collide with CuNP or adsorb copper ions released from CuNP, these ions can pass through the conduction channels and change the permeability of the cell wall, leading to the loss of mitochondrial membrane potential, opening of the permeability transition pore, formation of reactive oxygen species, and eventually cell death [30, 34].

3.7. Copper Release from CuNP/PET Filters during Filtration. Although copper is an essential trace element for human, an

excess of copper can cause health problems, such as abdominal pain, nausea, and diarrhea. Large amounts of copper in the body can cause gastrointestinal bleeding, anaemia, hepatocellular toxicity, and acute renal failure [35, 36]. Therefore, the release of CuNP from the antibacterial filters was investigated to ensure the safety of the filtrate based on published drinking water standards.

The amount of released copper after filtrating one liter of water through the 10 min filter was determined using ICP–MS was 0.6 ± 0.1 mg/L, which satisfies WHO drinking water standards (<2 mg/L). The low content of copper in the filtrate indicates a strong attachment of CuNP on the PET surface and a slow release of CuNP and copper ions upon filtration. However, further studies are needed to evaluate the copper release and the antibacterial effectiveness of CuNP/PET filters under practical conditions, such as repeated uses, pH, temperature, and the presence of other substances.

4. Conclusions

CuNP was chemically deposited on the surface of alkaline-treated PET filters by reducing $CuSO_4$ with ascorbic as the reducing agent and PVP as the capping agent. The influence of some synthetic conditions was evaluated and a CuNP/PET filter with a maximum antibacterial effect was attained using the one-factor-at-a-time approach. The copper released into the filtered water satisfies WHO standard for drinking water, which makes these filters promising for disinfection applications for point-of-use production of drinking water. Interestingly, reducing copper ions more than 10 min resulted in lower antibacterial effects possibly due to the conversion of Cu_2O to Cu, which was quickly oxidized in the air to CuO with low antibacterial capacity. This result suggests that producing and depositing Cu_2O nanoparticles on PET filters may lead to even more effective antibacterial filters with lower cost.

Data Availability

The data used to support the findings of this study are available from the corresponding author upon request.

Conflicts of Interest

The authors declare that there are no conflicts of interest regarding the publication of this paper.

Acknowledgments

The authors gratefully thank Ho Chi Minh City University of Technology and Education for facility supports in completing this research.

References

[1] WHO, *Progress on household drinking water, sanitation and hygiene 2000-2017: special focus on inequalities*, World Health Organization, 2019.

[2] S. V. Jadhav, E. Bringas, G. D. Yadav, V. K. Rathod, I. Ortiz, and K. V. Marathe, "Arsenic and fluoride contaminated groundwaters: a review of current technologies for contaminants removal," *Journal of Environmental Management*, vol. 162, pp. 306–325, 2015.

[3] E. Bahcelioglu, H. E. Unalan, and T. H. Erguder, "Silver-based nanomaterials: a critical review on factors affecting water disinfection performance and silver release," *Critical Reviews in Environmental Science and Technology*, pp. 1–35, 2020.

[4] V. T. Nguyen and K. S. Trinh, "Effects of synthetic procedures and postsynthesis incubation pH on size, shape, and antibacterial activity of copper (I) oxide nanoparticles," *Journal of Chemistry*, vol. 2020, Article ID 9541934, 10 pages, 2020.

[5] A. B. Rezaie and M. Montazer, "Polyester modification through synthesis of copper nanoparticles in presence of triethanolamine optimized with response surface methodology," *Fibers and Polymers*, vol. 18, no. 3, pp. 434–444, 2017.

[6] J. P. Ruparelia, A. K. Chatterjee, S. P. Duttagupta, and S. Mukherji, "Strain specificity in antimicrobial activity of silver and copper nanoparticles," *Acta Biomaterialia*, vol. 4, no. 3, pp. 707–716, 2008.

[7] J. Xiong, Y. Wang, Q. Xue, and X. Wu, "Synthesis of highly stable dispersions of nanosized copper particles using L-ascorbic acid," *Green Chemistry*, vol. 13, no. 4, pp. 900–904, 2011.

[8] S. Kumari, A. Panigrahi, S. Singh, and S. Pradhan, "Synthesis of graphene by reduction of graphene oxide using non-toxic chemical reductant," in *Innovation in Materials Science and Engineering*, pp. 143–150, Springer, 2019.

[9] L. Guo, W. Yuan, Z. Lu, and C. M. Li, "Polymer/nanosilver composite coatings for antibacterial applications," *Colloids and Surfaces A: Physicochemical and Engineering Aspects*, vol. 439, pp. 69–83, 2013.

[10] K. Dai, X.-B. Xu, and Z.-M. Li, "Electrically conductive carbon black (CB) filled in situ microfibrillar poly(ethylene terephthalate) (PET)/polyethylene (PE) composite with a selective CB distribution," *Polymer*, vol. 48, no. 3, pp. 849–859, 2007.

[11] E. Abdel-Halim, F. A. Abdel-Mohdy, S. S. al-Deyab, and M. H. el-Newehy, "Chitosan and monochlorotriazinyl-β-cyclodextrin finishes improve antistatic properties of cotton/polyester blend and polyester fabrics," *Carbohydrate Polymers*, vol. 82, no. 1, pp. 202–208, 2010.

[12] T. Spychaj, E. Fabrycy, S. Spychaj, and M. Kacperski, "Aminolysis and aminoglycolysis of waste poly (ethylene terephthalate)," *Journal of Material Cycles and Waste Management*, vol. 3, no. 1, pp. 24–31, 2001.

[13] D. M. Tomasiewicz, D. K. Hotchkiss, G. W. Reinbold, R. B. Read, and P. A. Hartman, "The most suitable number of colonies on plates for counting," *Journal of Food Protection*, vol. 43, no. 4, pp. 282–286, 1980.

[14] M. Arakha, M. Saleem, B. C. Mallick, and S. Jha, "The effects of interfacial potential on antimicrobial propensity of ZnO nanoparticle," *Scientific Reports*, vol. 5, no. 1, p. ???, 2015.

[15] J. De, N. Ramaiah, and L. Vardanyan, "Detoxification of toxic heavy metals by marine bacteria highly resistant to mercury," *Marine Biotechnology*, vol. 10, no. 4, pp. 471–477, 2008.

[16] V. T. Nguyen and K. S. Trinh, "In situ deposition of copper nanoparticles on polyethylene terephthalate filters and antibacterial testing against Escherichia coli and Salmonella enterica," *Brazilian Journal of Chemical Engineering*, vol. 36, no. 4, pp. 1553–1560, 2019.

[17] O. Ohiienko and Y. J. Oh, "New approach for more uniform size of Cu and Cu-CuO (core-shell) nanoparticles by double-

salt reduction," *Materials Chemistry and Physics*, vol. 218, pp. 296–303, 2018.

[18] D. Chattopadhyay and B. Patel, "Nano metal particles: synthesis, characterization and application to textiles," in *Manufacturing Nanostructures*, pp. 184–215, One Central Press (OCP), 2014.

[19] J. A. Lemire, J. J. Harrison, and R. J. Turner, "Antimicrobial activity of metals: mechanisms, molecular targets and applications," *Nature Reviews Microbiology*, vol. 11, no. 6, pp. 371–384, 2013.

[20] L. Chen, L. Zheng, Y. Lv et al., "Chemical assembly of silver nanoparticles on stainless steel for antimicrobial applications," *Surface and Coatings Technology*, vol. 204, no. 23, pp. 3871–3875, 2010.

[21] Y. Lee, J. R. Choi, K. J. Lee, N. E. Stott, and D. Kim, "Large-scale synthesis of copper nanoparticles by chemically controlled reduction for applications of inkjet-printed electronics," *Nanotechnology*, vol. 19, no. 41, p. 415604, 2008.

[22] D. S. Menamo, D. W. Ayele, and M. T. Ali, "Green synthesis, characterization and antibacterial activity of copper nanoparticles using L-ascorbic acid as a reducing agent," *Ethiopian Journal of Science and Technology*, vol. 10, no. 3, pp. 209–220, 2017.

[23] M. Hans, A. Erbe, S. Mathews, Y. Chen, M. Solioz, and F. Mücklich, "Role of copper oxides in contact killing of bacteria," *Langmuir*, vol. 29, no. 52, pp. 16160–16166, 2013.

[24] S. Meghana, P. Kabra, S. Chakraborty, and N. Padmavathy, "Understanding the pathway of antibacterial activity of copper oxide nanoparticles," *RSC Advances*, vol. 5, no. 16, pp. 12293–12299, 2015.

[25] H.-J. Park, T. T. M. Nguyen, J. Yoon, and C. Lee, "Role of reactive oxygen species in Escherichia coli inactivation by cupric ion," *Environmental Science & Technology*, vol. 46, no. 20, pp. 11299–11304, 2012.

[26] R. Borah, E. Saikia, S. J. Bora, and B. Chetia, "Banana pulp extract mediated synthesis of Cu_2O nanoparticles: an efficient heterogeneous catalyst for the _ipso_ -hydroxylation of arylboronic acids," *Tetrahedron Letters*, vol. 58, no. 12, pp. 1211–1215, 2017.

[27] M. Sabbaghan, J. Beheshtian, and R. Niazmand Liarjdame, "Preparation of Cu_2O nanostructures by changing reducing agent and their optical properties," *Materials Letters*, vol. 153, pp. 1–4, 2015.

[28] Z. Emami-Karvani and P. Chehrazi, "Antibacterial activity of ZnO nanoparticle on gram-positive and gram-negative bacteria," *African Journal of Microbiology Research*, vol. 5, no. 12, pp. 1368–1373, 2012.

[29] A. Sedighi, M. Montazer, and N. Samadi, "Synthesis of nano Cu2O on cotton: morphological, physical, biological and optical sensing characterizations," *Carbohydrate Polymers*, vol. 110, pp. 489–498, 2014.

[30] H. Li, Q. Chen, J. Zhao, and K. Urmila, "Enhancing the antimicrobial activity of natural extraction using the synthetic ultrasmall metal nanoparticles," *Scientific Reports*, vol. 5, no. 1, p. ???, 2015.

[31] A. F. Halbus, T. S. Horozov, and V. N. Paunov, "Controlling the antimicrobial action of surface modified magnesium hydroxide nanoparticles," *Biomimetics*, vol. 4, no. 2, p. 41, 2019.

[32] Y. He, S. Ingudam, S. Reed, A. Gehring, T. P. Strobaugh Jr., and P. Irwin, "Study on the mechanism of antibacterial action of magnesium oxide nanoparticles against foodborne pathogens," *Journal of Nanobiotechnology*, vol. 14, no. 1, p. 54, 2016.

[33] J. Li, Q. Li, X. Ma et al., "Biosynthesis of gold nanoparticles by the extreme bacterium Deinococcus radiodurans and an evaluation of their antibacterial properties," *International Journal of Nanomedicine*, vol. 11, pp. 5931–5944, 2016.

[34] T. Xia, M. Kovochich, and A. E. Nel, "Impairment of mitochondrial function by particulate matter (PM) and their toxic components: implications for PM-induced cardiovascular and lung disease," *Frontiers in Bioscience*, vol. 12, no. 1, p. 1238, 2007.

[35] S. Agarwal, S. C. Tiwari, and S. C. Dash, "Spectrum of poisoning requiring haemodialysis in a tertiary care hospital in India," *The International Journal of Artificial Organs*, vol. 16, no. 1, pp. 20–22, 1993.

[36] R. Eife, M. Weiss, V. Barros et al., "Chronic poisoning by copper in tap water: I. Copper intoxications with predominantly gastointestinal symptoms," *European Journal of Medical Research*, vol. 4, no. 6, pp. 219–223, 1999.

[37] A. K. Chatterjee, R. Chakraborty, and T. Basu, "Mechanism of antibacterial activity of copper nanoparticles," *Nanotechnology*, vol. 25, no. 13, p. 135101, 2014.

[38] Council, N R, "Size Limits of Very Small Microorganisms," in *Proceedings of a Workshop: National Academies Press*, US, 1999.

[39] T. A. Dankovich, J. S. Levine, N. Potgieter, R. Dillingham, and J. A. Smith, "Inactivation of bacteria from contaminated streams in Limpopo, South Africa by silver-or copper-nanoparticle paper filters," *Environmental Science: Water Research & Technology*, vol. 2, no. 1, pp. 85–96, 2016.

[40] T. A. Dankovich and J. A. Smith, "Incorporation of copper nanoparticles into paper for point-of-use water purification," *Water Research*, vol. 63, pp. 245–251, 2014.

[41] Y.-L. Hsieh, A. Miller, and J. Thompson, "Wetting, pore structure, and liquid retention of hydrolyzed polyester fabrics," *Textile Research Journal*, vol. 66, no. 1, pp. 1–10, 2016.

[42] J. H. Yoe and C. J. Barton, "Colorimetric determination of copper with triethanolamine," *Industrial & Engineering Chemistry Analytical Edition*, vol. 12, no. 8, pp. 456–459, 1940.